Bulletin of Pure and Applied Sciences
Section - E - Mathematics & Statistics
Website : https : //www.bpasjournals.com/

Bull. Pure Appl. Sci. Sect. E Math. Stat.
38E(2), 570–585 (2019)
e-ISSN:2320-3226, Print ISSN:0970-6577
DOI: 10.5958/2320-3226.2019.00058.4

Unsteady and steady non-linear state flow of Burgers' fluid in the presence of magnetic field with heat generation/absorption *

P.H. Nirmala[1] and A. Saila Kumari[2]

1. Research Scholar, Department of Mathematics, JNTU University,
Ananthapur-515002, Andhra Pradesh, India.
2. Assistant Professor, Department of Mathematics, JNTU University,
Ananthapur-515002, Andhra Pradesh, India.
1. E-mail: nirmalaph83@gmail.com , 2. E-mail: asailakumari@gmail.com

Abstract This paper describes the theoretical analysis of unsteady non-linear convection of magnetic field effect on Burgers' fluid flow in the presence of Buongiorno nano model. The flow is created by stretching the surface. Diffusion of thermal, concentration levels and heat absorption/generation are examined. Suitable similarity transformations are used to convert the nonlinear partial differential system into the nonlinear ordinary differential system. The solutions of nonlinear systems are obtained from the convergent approach. The profiles temperature, concentration and velocity are elaborated by various physical flow parameters and these are investigated through the graphs. Local Nusselt and Sherwood numbers numerical values are interpreted and discussed for various values of physical parameters in the form of the table. In the following research we determine the velocity, temperature, and concentration are extremely clear with the flow in non-linear unsteady convection than in the non-linear steady convection and also observe that the cooling process of non-linear unsteady convection is exceedingly beneficial.

Key words Magnetohydrodynamic, stretched sheet, Brownian motion, Buongiorno nanomodel, Nusselt number, Sherwood number, steady convection, unsteady convection.

2010 Mathematics Subject Classification 76W05, 76W99.

1 Introduction

The analysis of Nanofluids plays a major role in the research because the improvement of heat transfer technique rate is needed for the industrial requirements. The reason behind the argument is that those industrial manufacturing processes which need a higher rate of heat transfer, for them the normal heat transfer techniques fail to yield the desired outcomes as per the industrial requirements. Nanofluids are used for the progress of the physical properties particularly with regard to heat transfer. These fluids are the combination of a base liquid and nanoparticles. Many researchers have studied the mixture and the impact of liquid-solid for enhancing the heat transfer rate. Altiparmak and Turgut [1] found out the numerical solution of Burgers' fluid equation with the factorized diagonal calculation. Choi

* Communicated, edited and typeset in Latex by *Lalit Mohan Upadhyaya* (Editor-in-Chief).
Received December 11, 2018 / Revised May 21, 2019 / Accepted June 27, 2019. Online First Published on December 24, 2019 at https://www.bpasjournals.com/.
Corresponding author P.H. Nirmala, E-mail: nirmalaph83@gmail.com

and Eastman [2] were the first to propose the word Nanofluid. They reported thermal conductivity enhancement dramatically by scattering tiny sized solid particles in base liquids. Khan et al. [3] investigated the fractional Burgers' model in the viscoelastic fluid with an accelerated flow. The unsteady flow of a viscoelastic fluid with fractional Burgers' model was studied by Ali and Shah [4]. Shah and Ali [5] applied the fractional derivative technique to study the unsteady flows of a viscoelastic fluid using Burgers' model. Jamil and Fetecau [6] examined the exact solutions of a Burgers' fluid over a cylindrical domain of rotating flow.

The study of non-Newtonian fluids with boundary layer flows made by a constantly moving surface is a great interest area of research for the researchers owing to their extensive attempts of concrete applications in engineering and industry. In this aspect, the research has been going on for the past many years due to the application of pharmaceutical, chemical, food and biological industries. Many non-Newtonian fluids are used as industrial fluids such as polymers, ice creams, shampoos, paper pulp, paints, ketchup, certain oils, colloidal fluids, cosmetic products etc. Khan et al. [7] analyzed the exact solution for non-Newtonian fluid model of unsteady flow in motion of one the plates between couple of sidewalls perpendicular to plate and found out this solution using the Fourier sine transforms. Liu et al. [8] have discussed the thermal radiation and magnetic field effects influence on the Burgers' fluid flow in accelerating plate. Narayana and Sibanda [9] investigated two altered types of unsteady nano liquids flow at stretching sheet. Dengke et al. [10] presented a fractional derivative based analysis of the exact solutions for the non-Newtonian fluid model flow in an annular pipe. Xu et al. [11] studied a thermal processing of unsteady film nano-fluid flow over an unsteady stretching sheet.

The occurrence of heat transfer takes place if there is variance in temperature between the components or between the related bodies. This phenomenon is useful in industrial and technological procedures. At present, the research is on Burgers' fluid model because its application is involved in extensive engineering and industrial applications, such as plastic manufacturing, thinning and annealing of copper wires, drawing of the stretching sheet through the quiescent fluid and aerodynamic extrusion of the plastic films etc. The famous Navier-Stokes equations are much more difficult in controlling the non-Newtonian material flows. A distinct relation is not enough to depict the physical characteristics of all non-Newtonian materials. Therefore, the following literature discusses different types of non-Newtonian material relations. The Burgers' expression has been studied comprehensively both numerically and theoretically. The Burgers' expression is a simple way to understand the important properties of Navier-Stokes equations. Between these relations, Burgers' fluid model [12] – [18] is the sub-class of rate type fluids and it was proposed to expect the properties of retardation and relaxation time.

Recently, the researchers have been focusing on the study of magnetohydrodynamic flow persuading heat transfer in different geometrical figures. The investigation of flow and heat transfer of the electrically conducting fluids in numerous channels is of great theoretical interest because of its application in astrophysical phenomena and a variety of geophysical situations. Seth and Mishra [19] investigated the effects of thermal radiation and velocity slip of MHD nanofluid flow over the nonlinear stretching sheet. Thumma et al. [20] presented the heat sink/source effects on MHD nanofluid flow from shrinking/stretching sheet numerically. Nirmala et al. [21] analyzed the pressure and velocity of unsteady magnetohydrodynamic flow among two parallel plates. Rashidi et al. [22] generalized the physical characteristics of MHD Burgers' fluid model flow. Nirmala et al. [23] investigated the heat and mass transfer of MHD natural convection flow over the vertical surface in porous media. Adila et al. [24] analyzed the boundary layer stagnation-point nanofluid flow with mixed convection over the vertical shrinking/stretching surface.

Our aim here is to examine the characteristics of unsteady nonlinear convection in the MHD flow of Burgers' fluid over a stretching surface in the presence of Buongiorno nano model with the dissipation effect. The Brownian motion and thermophoresis effects are also taken into consideration. The effects of various parameters on fluid temperature, velocity and concentration are shown graphically. We hope that our analysis will be useful for the purpose of various applications in this field and we also mention that it gives an excellent agreement with the result of the previous studies.

2 Problem progresses

We study the time-dependent solutions of the equations governing the unsteady non-linear convection in the magnetohydrodynamic flow of Burgers' nanofluid and also consider the thermal effect and con-

centration effect stratifications with the generation or absorption of heat. Let T_w be the temperature at a sheet and T_∞ be the temperature away from the sheet. Similarly, let C_w be the concentrate at the sheet and C_∞be the concentrate away from the sheet.
Considering the stretching sheet velocity $u_w = \frac{ax}{1-ct}$, let a be the initial stretching rate and c be the unsteadiness positive constant measuring the Brownian motion. The thermophoresis and dissipation attributes are also taken into account. Here the stretching sheet is taken along the $x-$ axis and its normal along the $y-$ axis. The governing equations of an incompressible Burgers' fluid for two-dimensional motion are

$$\mathrm{div}V = 0 \tag{2.1}$$

where $V = V(u, v, w), w = 0, u = u(x, y), v = v(x, y)$

$$\frac{dV}{dt} = \frac{1}{\rho}\mathrm{div}C_T \tag{2.2}$$

The Cauchy stress tensor (C_T) of Burgers' fluid is

$$C_T = -pI + E_S \tag{2.3}$$

and the extra stress tensor E_S is

$$\left(1 + t_1\frac{D}{Dt} + t_2\frac{D^2}{Dt^2}\right)E_S = \mu\left(1 + t_3\frac{D}{Dt}\right)A_1 \tag{2.4}$$

in which the operator $\frac{D}{Dt}$ denotes the upper convicted derivative defined by $\frac{D}{Dt} = \frac{\partial a_i}{\partial t} + u_r a_{i,r} - u_{i,r}a_i$, p is the pressure, the times relaxation and retardation parameters are $t_1$and t_3, the dynamic viscosity parameter is μ and t_2 is the Burgers' fluid material parameter.
The Rivlin-Erickson tensor A_1 is represented by

$$A_1 = (\nabla V) + (\nabla V)^\lambda \tag{2.5}$$

where λ is the matrix transpose, $\frac{\partial a_i}{\partial t}$ is defined as

$$\frac{\partial a_i}{\partial t} = \frac{\delta a_i}{\delta t} - u_r a_{i,r} + u_{i,r}a_r \tag{2.6}$$

The governing equations of the unsteady nonlinear Burgers' fluid in the presence of magnetic field, convection and dissipation, Brownian motion and thermophoresis attributes are taken into cosideration in the energy equation.
Continuity

$$\frac{\partial u}{\partial x} + \frac{\partial v}{\partial y} = 0 \tag{2.7}$$

Momentum

$$\begin{aligned}
&\frac{\partial u}{\partial t} + u\frac{\partial u}{\partial x} + v\frac{\partial u}{\partial y} + t_1\left(u^2\frac{\partial^2 u}{\partial x^2} + 2uv\frac{\partial^2 u}{\partial x\partial y} + v^2\frac{\partial^2 u}{\partial y^2}\right) + \\
&t_2\begin{bmatrix}\left(u^3\frac{\partial^3 u}{\partial x^3} + v^3\frac{\partial^3 u}{\partial y^3}\right) + u^2\left(\frac{\partial u}{\partial x}\frac{\partial^2 u}{\partial x^2} + 2\frac{\partial v}{\partial x}\frac{\partial^2 u}{\partial x\partial y} - \frac{\partial u}{\partial y}\frac{\partial^2 v}{\partial x^2}\right) + \\ 2uv\left(\frac{\partial u}{\partial y}\frac{\partial^2 u}{\partial x^2} + \frac{\partial v}{\partial y}\frac{\partial^2 u}{\partial x\partial y} + \frac{\partial v}{\partial x}\frac{\partial^2 u}{\partial y^2} - \frac{\partial u}{\partial y}\frac{\partial^2 v}{\partial x\partial y}\right) + \\ 3uv\left(u\frac{\partial^3 u}{\partial x^2\partial y} + v\frac{\partial^3 u}{\partial x\partial y^2}\right) + 3v^2\left(\frac{\partial u}{\partial y}\frac{\partial^2 u}{\partial x\partial y} + \frac{\partial v}{\partial y}\frac{\partial^2 u}{\partial y^2}\right)\end{bmatrix} \\
&-\frac{\sigma\beta_0^2}{\rho}u = \upsilon\left[\frac{\partial^2 u}{\partial y^2} + t_3\left(v\frac{\partial^3 u}{\partial y^3} - \frac{\partial u}{\partial x}\frac{\partial^2 u}{\partial y^2} + u\frac{\partial^3 u}{\partial x\partial y^2} - \frac{\partial u}{\partial y}\frac{\partial^2 v}{\partial y^2}\right)\right] \\
&+\left[g\beta\left(T - T_\infty\right) + g\beta(T - T_\infty)^2 + g\beta_c\left(C - C_\infty\right) + g\beta_c(C - C_\infty)^2\right]
\end{aligned} \tag{2.8}$$

Energy

$$\frac{\partial T}{\partial t} + u\frac{\partial T}{\partial x} + v\frac{\partial T}{\partial y} = T_D\frac{\partial^2 T}{\partial y^2} + \tau\left[D_{Br}\frac{\partial C}{\partial y}\frac{\partial T}{\partial y} + \frac{D_T}{T_\infty}\left(\frac{\partial T}{\partial y}\right)^2\right] + \frac{\mu}{\rho C_p}\left(\frac{\partial u}{\partial y}\right)^2 \tag{2.9}$$

Concentration

$$\frac{\partial C}{\partial t}+u\frac{\partial C}{\partial x}+v\frac{\partial C}{\partial y}=\left[D_{Br}\frac{\partial^2 C}{\partial y^2}+\frac{D_T}{T_\infty}\left(\frac{\partial^2 T}{\partial y^2}\right)\right] \tag{2.10}$$

The subjected flow model boundary conditions are

$$\begin{aligned}&\text{if } y=0 \text{ then } u=U_w, v=0, T=T_w, C=C_w;\\ &\text{if y } \to\infty \text{ then } u\to 0, T\to T_\infty, C\to C_\infty.\end{aligned} \tag{2.11}$$

where υ is the kinematic viscosity, $T_D=\frac{k}{\rho C_p}$ thermal diffusivity, (D_{Br}, D_T) the Brownian and thermophoresis diffusion coefficient, k the thermal conductivity and C_p the specific heat.
The equations (2.7), (2.8), (2.9) and (2.10) are converted into dimensionless form by using the following similarity variables

$$\begin{aligned}&u=\tfrac{ax}{1-ct}f^1(\eta), v=\left(-\tfrac{a\upsilon}{1-ct}\right)^{\frac{1}{2}}f(\eta), \eta=y\left(\tfrac{a}{\upsilon(1-ct)}\right)^{\frac{1}{2}}\\ &T=(T_w-T_\infty)\theta(\eta)+T_\infty, C=(C_w-C_\infty)\phi(\eta)\end{aligned} \tag{2.12}$$

The continuity equation is satisfied and the other equations viz., momentum, energy and concentration are in the following form

$$f^{iv}=\left(1/\left(\beta_2 f^3-\beta_3 f\right)\right)\left[\begin{array}{l}Af'+0.5A\eta f''+f'^2-ff''-\beta_1 f^2 f'''+6\beta_2 f^2 f' f'''-Mf'\\ -f'''-\beta_3 f''^2-S_1(\theta+N\phi)-S_2\left(\theta^2+N^2\phi^2\right)\end{array}\right] \tag{2.13}$$

$$\theta''=(0.5\,\mathrm{Pr}\,\eta A\theta'-\mathrm{Pr}\,f\theta'-\mathrm{Pr}\,Nb\theta'\phi'-\mathrm{Pr}\,Nt\theta'^2-\mathrm{Pr}\,Ecf''^2) \tag{2.14}$$

$$\phi''=\left(0.5\eta AS_c\phi'-S_c f\phi'-\frac{Nt}{Nb}S_c\theta''\right) \tag{2.15}$$

The transformed boundary conditions are as follows

$$\begin{aligned}&f(0)=0, f'(0)=1, \theta(0)=1, \phi(0)=1\\ &f(\infty)=0, f'(\infty)=0, \theta(\infty)=0, \phi(\infty)=0\end{aligned} \tag{2.16}$$

where A is the unsteadiness parameter, M is the Magnetic parameter, (S_1, S_2, S_3) is the buoyancy and nonlinear convection parameter, N is the thermo buoyancy effect, (β_1, β_3) are Deborah numbers and β_2 is the viscoelastic fluid particle interaction parameter for temperature, P_r is the Prandtl number, N_b is the Brownian motion parameter, N_t is the thermophoresis parameter, E_C is the Eckert number. The representations of the used parameters are:

$$\begin{aligned}&A=\tfrac{c}{a}, M=\tfrac{\sigma\beta_0^2(1-ct)}{a\rho}, Re_x=\tfrac{U_w x}{\upsilon}, E_C=\tfrac{U_w^2}{(T_w-T_\infty)C_p}, \upsilon=\tfrac{\mu}{\rho}, P_r=\tfrac{\upsilon}{\alpha}, S_C=\tfrac{T_D}{D_B},\\ &N_b=\tfrac{D_{Br}\tau(C_w-C_\infty)}{\upsilon}, N_t=\tfrac{D_T\tau(T_w-T_\infty)}{T_\infty\upsilon}, \beta_1=\tfrac{t_1 a}{(1-ct)}, \beta_2=\tfrac{t_2 a^2}{(1-ct)^2}, \beta_3=\tfrac{at_3}{(1-ct)},\\ &N=\tfrac{\beta_C(C_w-C_\infty)}{\beta_T(T_w-T_\infty)}, Gr_x=\tfrac{g\beta_T(T_w-T_\infty)x^3}{\upsilon^2}, S_1=\tfrac{Gr_x}{Re_x^2}, S_2=S_1S_3, S_3=\tfrac{\beta_T(T_w-T_\infty)}{\beta_C^2}\end{aligned} \tag{2.17}$$

where Re_x is the local Reynolds number and Gr_x is the local Grashoff number.
It observed that the results of the viscous fluid can be obtained by taking $\beta_1=\beta_2=\beta_3=0$.
The heat and concentration rates are defined as follows:

$$Nu_x=\frac{-x}{(T_w-T_0)}\left(\frac{\partial T}{\partial y}\right)|_{y=0} \tag{2.18}$$

$$Nu_x/Re_x^{0.5}=-\theta^1(0) \tag{2.19}$$

$$Sh_x=\frac{-x}{(C_w-C_0)}\left(\frac{\partial C}{\partial y}\right)|_{y=0} \tag{2.20}$$

$$Sh_x/Re_x^{0.5}=-\phi^1(0) \tag{2.21}$$

Below we provide a consolidated complete list of the various symbols used by us in this work for a ready reference of the interested reader:

Nomenclature

a, Initial stretching rate;
A, unsteadiness parameter;
A_1,Rivlin-Erickson tensor;
c, Unsteadiness positive constant measure;
C, Concentration;
C_w,Concentration at the wall;
C_∞, Concentration at infinity;
C_T,Cauchy stress tensor;
C_p,Specific heat;
D_{Br}, Brownian diffusion coefficient;
D_T, thermophoresis diffusion coefficient;
E_C,the Eckert number;
E_S,Extra stress tensor;
g, Acceleration due to gravity;
Gr_x,Local Grashoff number ;
f, Dimensionless stream function;
k, Effective thermal conductivity;
N,Buoyancy ratio;
N_b, Brownian motion parameter;
N_t,thermophoresis parameter;
Nu,Nusselt number;
M, Magnetic field;
p, Pressure;
P_r, Prandtl number;
Re_x,Local Reynolds number;
(S_1, S_2, S_3),Buoyancy and nonlinear convection parameter;
Sh,Sherwood number;
t_1, Time parameter relaxation;
t_2, Time parameter retardation;
t_3, Burgers' fluid material parameter;
T, Temperature;
T_w,Temperature at the wall;
T_∞, Temperature at infinity;
T_D,Thermal diffusivity of porous medium;
u, velocity in the $x-$ direction;
v, velocity in the $y-$ direction.

Nomenclature Greek symbols

(β_1, β_3)Deborah number;
β_2, Viscoelastic of fluid particle;
β_C,Coefficient of concentration expansion;
β, Coefficient of thermal expansion;
λ, The matrix transpose;
η, Independent similarity variable;
μ, The dynamic viscosity parameter;
υ, Kinematic viscosity of convective fluid;
θ, Dimensionless temperature;
ϕ , Dimensionless concentration;
ρ, Density of convective fluid;
σ, Electrical conductivity of the fluid;
β_0^2, Electromagnetic field.

Nomenclature Subscript

w, Condition at the wall;
∞, Condition at infinity.

3 Numerical, Graphical outcomes and discussion

The converted set of equations (2.13) to (2.15) are highly unsteady non-linear equations and subject to a two-point boundary value problem. The equations (2.13) to (2.15) are solved numerically with boundary conditions (2.16) using the shooting method in the MATLAB software. The flow and heat transfer are analyzed graphically. The results of the present problem are understood based on the tabular values and graphical representations. The previous publications [14,16,17] and [12] studied the Burgers' fluid in a steady flow, while in the present paper we analyze the Burgers' fluid in unsteady flow in the presence of magnetic field. The accuracy of the numerical computations of this study of ours is repetitively confirmed with previous publications [12–16] and [17], which is the strength of this work. We further compare below the unsteady non-linear flow with the steady non-linear flow graphically. Table 1 (Fig. 1) and Table 2 (Fig. 2) show the comparison of unsteady and steady non-linear Burgers' fluid flow in the presence of magnetic field. In Table 1 (Fig. 1) numerically we observe the Nusselt number (denoted by the word 'Nur') and skin friction variation. We can also analyze the flow and the time taken for execution in seconds. The time taken for the execution in unsteady flow is less than the steady flow, which means that the flow is very smooth and numerically accurate in unsteady flow than in the steady flow. In the same way, we present the comparison of the numerical values of skin friction

M	N	N_t	N_b	E_C	S_C	$A=1$			$A=0$		
						Skin	Nur	Time taken for execution (seconds)	Skin	Nur	Time taken for execution (seconds)
0.1						-5.3486	-0.0184	3.373373	-3.7778	-0.0127	4.007209
0.2						-4.2118	-0.0123		-2.6810	-0.0041	
0.3						-3.3825	-0.0077		-2.8202	0.00519	
	0.5					-3.5869	-0.0064	2.538032	-2.3025	0.02669	3.354812
	1					-4.1366	-0.0105		-2.7731	0.00545	
	1.5					-4.8494	-0.0152		-3.4215	-0.0076	
		0.1				-5.8616	-0.0125	2.92085	-4.5055	-0.0061	3.900206
		0.2				-5.8461	-0.0124		-4.4861	-0.0059	
		0.3				-5.8304	-0.0123		-4.4666	-0.0056	
			0.1			-4.5305	0.02188	2.41083	-3.7271	0.10212	2.315726
			0.2			-4.6126	0.01964		-3.7786	0.09757	
			0.3			-4.6418	0.01854		-3.7990	0.09481	
				0.01		-5.8878	-0.0214	3.91644	-3.8355	0.10338	24.81031
				0.05		-5.9078	-0.1086		-0.4328	0.32943	
				0.1		-5.9337	-0.2191		-1.9479	0.32984	
					0.5	-5.9192	-0.0217	3.53375	-3.8517	0.09654	4.24353
					0.7	-5.9264	-0.0217		-3.8922	0.09166	
					0.9	-5.9293	-0.0217		-3.9527	0.08723	

Fig. 1: **Table1:** Distinction of friction factor and Nusselt number in unsteady ($A=1$) and steady ($A=0$) non-linear flow.

and Sherwood number (denoted by the word 'shr') in Table 2 (Fig. 2) and observe that the steady flow of skin friction and concentration is more than the unsteady flow and it takes more time.

Our primary goal, in this article, is to examine the characteristics of various sundry parameters on temperature, velocity and concentration distributions in the presence of magnetic field. This goal is achieved here by plotting the reults in Figs. 3 – 17. The influence of magnetic field parameter M of unsteady non-linear Burgers' fluid on $f'(\eta)$, $\theta(\eta)$, $\phi(\eta)$ are explored in the Figs. 3 – 5. It shows that the larger values of M cause a decrease in the dimensionless velocity ($f'(\eta)$) and rise in the temperature and concentration. Consequently the Lorentz force exists and the impact of magnetic field on velocity, both in the unsteady and the steady flows can be seen. Thermal boundary layer is enhanced for larger value of M. But we observe that the flow is very smooth, accurate and consumes less time for execution in unsteady flow than in the steady flow.

Figs. 6, 7 and 8 illustrate the influence of the Brownian motion parameter N_b on $f'(\eta)$, $\theta(\eta)$, $\phi(\eta)$. We see that the thermal boundary layer, temperature and concentration are enhanced for the higher value of N_b and an exactly opposite trend is observed for the velocity.

The investigation for the effect of thermophoresis parameter N_t is shown in Figs. 9, 10 and 11. Generally, thermophoresis is a mechanism of pulling little particles far away from the hot surface to a reserved one. The temperature distribution enhances and the behavior of velocity and concentration are opposite for higher values of thermophoresis parameter. Based on the graphs, we observe that the

M	N	N_t	N_b	E_C	S_C	$A=1$			$A=0$		
						Skin	shr	Time taken for execution (seconds)	Skin	shr	Time taken for execution (seconds)
0.1						-5.3486	0.00197	3.373373	-3.7778	0.00286	4.007209
0.2						-4.2118	0.00140		-2.6810	0.00543	
0.3						-3.3825	0.00123		-2.8202	0.01658	
	0.5					-3.5869	0.00519	2.538032	-2.3025	0.03998	3.354812
	1					-4.1366	0.00335		-2.7731	0.01875	
	1.5					-4.8494	0.00240		-3.4215	0.00692	
		0.1				-5.8616	0.00194	2.92085	-4.5055	0.00309	3.900206
		0.2				-5.8461	0.00368		-4.4861	0.00531	
		0.3				-5.8304	0.00544		-4.4666	0.00757	
			0.1			-4.5305	0.05845	2.41083	-3.7271	0.13472	2.315726
			0.2			-4.6126	0.04566		-3.7786	0.12359	
			0.3			-4.6418	0.04140		-3.7990	0.11957	
				0.01		-5.8878	0.00233	3.91644	-3.8355	0.12294	24.81031
				0.05		-5.9078	0.01041		-0.4328	0.27687	
				0.1		-5.9337	0.02066		-1.9479	0.28808	
					0.5	-5.9192	0.00330	3.53375	-3.8517	0.11963	4.24353
					0.7	-5.9264	0.00445		-3.8922	0.10995	
					0.9	-5.9293	0.00553		-3.9527	0.09564	

Fig. 2: **Table 2:** Distinction of friction factor and Sherwood number in unsteady and steady non-linear flow.

error free values and behavior of fluid at boundary layer are in good agreement with the unsteady flow than in the steady flow.

Figs. 12, 13 and 14 illustrate the buoyancy effect on $f'(\eta)$, $\theta(\eta)$, $\phi(\eta)$ fields. Clearly, we see that the heat and mass transfer rates raise and depreciate at the velocity field. The analysis of the effect of Eckert number parameter E_C on temperature field is displayed in the Fig. 15. Subsequently, the temperature and boundary layer are boosted for larger E_C.

The characteristic of the Deborah number β_1 on velocity, temperature, and concentration fields are explored in Figs. 16, 17 and 18. Fig. 19 and 20 illustrate the characteristics of Schmidt number on temperature and concentration field. Thermal distribution is very accurate with smooth fluid flow in the unsteady flow than that in the steady flow. The same way more flow fluctuations S_C are seen in the concentration field in the steady flow, but in unsteady flow, the fluid flow is very smooth and values are accurate. Similar features are found existing at the temperature field in a steady flow and unsteady flow with a proper fluid flow.

Theoretically, the influence of $A = 1$ value improves the thermal boundary layer and the temperature distribution in the flow and velocity boundary layer are reduced compared to $(A = 0)$. Therefore, the fluid flow in the unsteady flow condition $(A = 1)$ is proper, smooth with an accurate value better than the steady flow $(A = 0)$.

4 Conclusion

In the mainstream of the science, engineering and industrial process, convection is non-linear. It has various applications such as high surface area, stability and electron mobility. In an assessment of this in the present analysis, we compared the Burgers' fluid flow in unsteady and steady convection in the presence of magnetic field. The computational results for no dimensional velocity, temperature, and concentration profiles are offered through graphs in the following cases$A = 0$ and $A = 1$. Moreover, the numerical values of heat transfer and friction factor are compared in non-linear unsteady and steady flows over a stretching sheet. Similarly the numerical values of mass transfer and friction factor are calculated for the non-linear unsteady and the steady flows and they are tabulated numerically for various physical parameters obtained. The highlights of this analysis are:

- The thermophoresis and Brownian motion parameter are to be separate for the different particles in the field flow friction, we can highlight this in unsteady flow to control the flow.
- The time in use for the execution in the presence of non-linear unsteady convection is very less compared to non-linear steady convection fluid flow.
- The velocity, temperature, and concentration are extremely clear with the flow in non-linear unsteady convection than in the non-linear steady convection. With this, we determine that the cooling process of non-linear unsteady convection is exceedingly beneficial.
- The heat transfer, skin friction, and mass transfer rate are found extremely minor in non-linear unsteady convection compared to the non-linear steady convection.

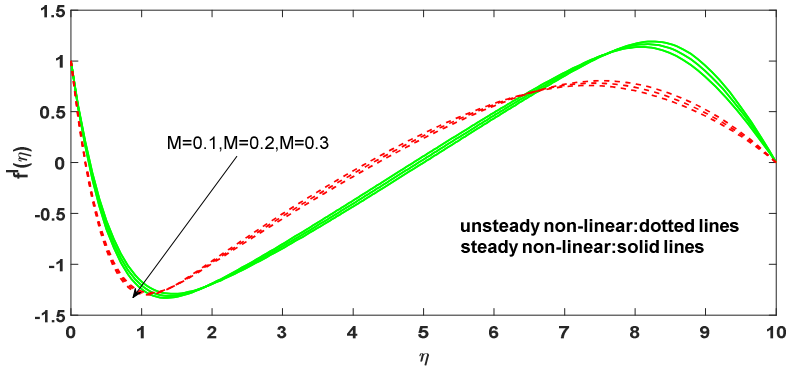

Fig. 3: Effect of the Magnetic field M on temperature profiles $\theta(\eta)$ when $\Pr = 0.3, M = 0.5, A = 0.2, \beta_1 = \beta_2 = \beta_3 = 0.2, t_1 = t_2 = 0.2, N_t = 0.1, N_b = 0.3, E_c = 0.01, S_c = 0.3$ and $N = 2$ are fixed.

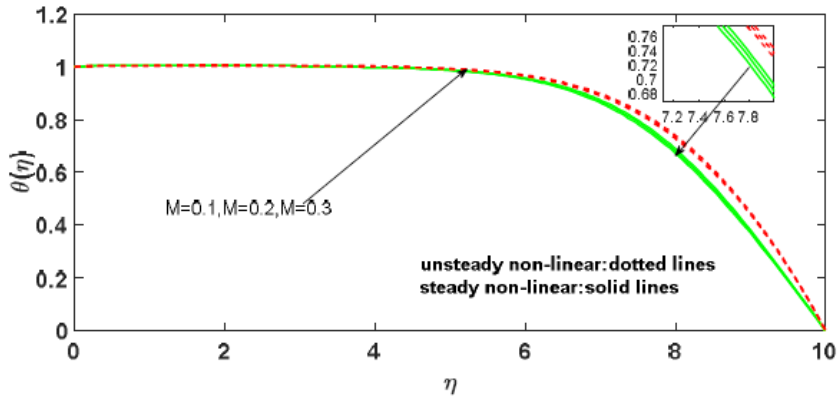

Fig. 4: Effect of the Magnetic field M on temperature profiles $\theta(\eta)$ when $\Pr = 0.3, M = 0.5, A = 0.2, \beta_1 = \beta_2 = \beta_3 = 0.2, t_1 = t_2 = 0.2, N_t = 0.1, N_b = 0.3, E_c = 0.01, S_c = 0.3$ and $N = 2$ are fixed.

References

[1] Altiparmak, Kemal and Turgut, Özis (2011), Numerical solution of Burgers' equation with factorized diagonal approximation Padé, *International Journal of Numerical Methods for Heat & Fluid Flow*, 21(3), 310–319. doi.org/10.1108/09615531111108486.

[2] Choi, S.U.S. and Eastman, J.A. (1995). Enhancing thermal conductivity of fluids with Nanoparticles, Conference: 1995 International Mechanical Engineering Congress and Exhibition, San Francisco, CA (United States), 12–17 November, 1995.

[3] Khan, M., Ali, S.H. and Qi, H. (2009). Nonlinear Analysis: Real World Applications on accelerated flows of a viscoelastic fluid with the fractional Burgers' model, 10, 2286–2296. doi:10.1016/j.nonrwa.2008.04.015.

[4] Ali, S.H. and Shah, M. (2010). Some helical flows of a Burgers' fluid with fractional derivative, 143–151, doi:10.1007/s11012-009-9233-z.

[5] Ali, S.H. and Shah, M. (2010). Nonlinear Analysis: Real World Applications Unsteady flows of a viscoelastic fluid with the fractional Burgers' model, 11, 1714–1721. doi:10.1016/j.nonrwa.2009.03.026.

[6] Jamil, M. and Fetecau, C. (2010). Some exact solutions for rotating flows of a generalized Burgers' fluid in cylindrical domains, *Journal of Non-Newtonian Fluid Mechanics*, 165, 1700–1712. doi:10.1016/j.jnnfm.2010.08.004.

[7] Khan, M., Malik, R. and Fetecau, C. (2010). Exact solutions for the unsteady flow of a Burgers' fluid between two sidewalls perpendicular to the plate, 1367–1386. doi:10.1080/00986441003626078.

[8] Liu, Y., Zheng, L. and Zhang, X. (2011). MHD flow and heat transfer of a generalized Burgers' fluid due to an exponential accelerating plate with the effect of radiation, 62 (2011) 3123–3131. doi:10.1016/j.camwa.2011.08.025.

[9] Narayana, M. and Sibanda, P. (2012). Laminar flow of a nanoliquid film over an unsteady stretching sheet, *International Journal of Heat and Mass Transfer*, 55, 7552–7560.

[10] Dengke, T., Ruihe, W. and Heshan, Y. (2005). Exact solutions for the flow of non-Newtonian fluid with fractional derivative in an annular pipe, *Science in China Ser. G Physics, Mechanics & Astronomy*, 48(4), 485–495. doi:10.1360/04yw0105.

[11] Xu, H., Pop, I. and You, X. (2013). Flow and heat transfer in a nano-liquid film over an unsteady stretching surface, *International Journal of Heat and Mass Transfer*, 60, 646–652.

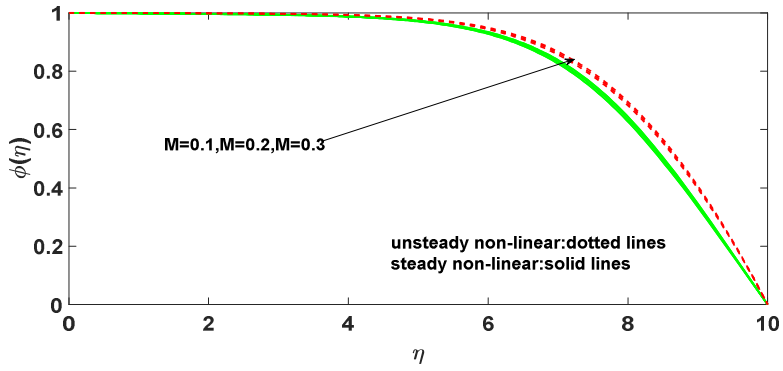

Fig. 5: Effect of the Magnetic field M on concentration profiles $\phi(\eta)$ when $\Pr = 0.3, M = 0.5, A = 0.2, \beta_1 = \beta_2 = \beta_3 = 0.2, t_1 = t_2 = 0.2, N_t = 0.1, N_b = 0.3, E_c = 0.01, S_c = 0.3$ and $N = 2$ are fixed.

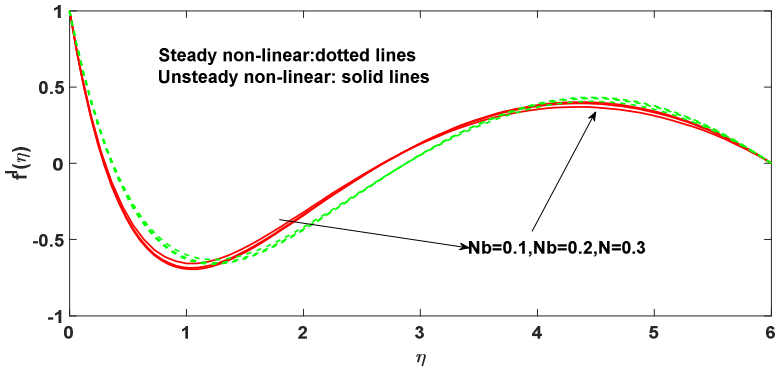

Fig. 6: Effect of the N_b on velocity with the following fixed values $\Pr = 0.3, M = 0.5, A = 0.2, \beta_1 = \beta_3 = 0.2, \beta_2 = 0.3, t_1 = t_2 = 0.2, N_t = 0.1, N_b = 0.3, E_c = 0.01, S_c = 0.3$ and $N = 2$.

[12] Khan, M. and Azeem, W. (2014). Steady flow of Burgers' nanofluid over a stretching surface with heat generation/absorption, *The Brazilian Society of Mechanical Sciences and Engineering*, 38(8), 2359–2367. doi.org/10.1007/s40430-014-0290-4.

[13] Awais, M., Hayat, T. and Alsaedi, A. (2015). Investigation of heat transfer in flow of Burgers' fluid during a melting process, *Journal of the Egyptian Mathematical Society*, 23(2), 410–415.doi.org/10.1016/j.joems.2014.04.004.

[14] Khan, M. and Khan, W.A. (2015). Forced convection analysis for generalized Burgers' nanofluid flow over a stretching sheet, *AIP Advances*, 5, 107138 (2015). doi.org/10.1063/1.4935043.

[15] Han, S. and Zheng, L. (2016). Slip effects on a generalized Burgers' fluid flow between two side walls with fractional derivative, *Journal of the Egyptian Mathematical Society*, 24, 130–137. doi.org/10.1016/j.joems.2014.10.004.

[16] Hayat, T., Waqas, M., Shehzad, S.A. and Alsaedi A. (2016). Mixed convection flow of a Burgers' nanofluid in the presence of stratifications and heat generation/absorption, *The European Physical Journal Plus*, 131(8), 253. doi:10.1140/epjp/i2016-16253-9.

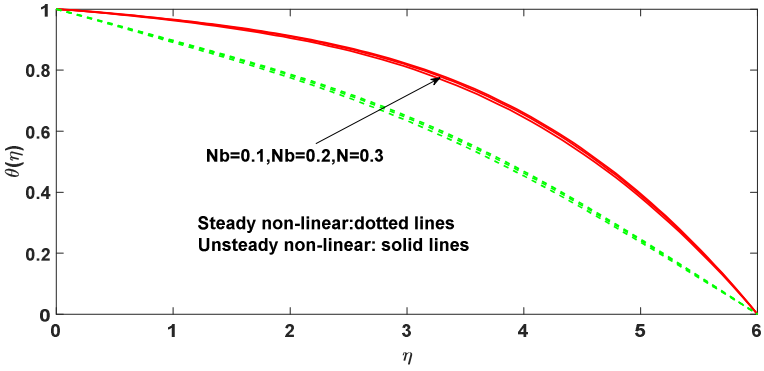

Fig. 7: Effect of the N_b on temperature profile $\theta(\eta)$ with the following fixed values $\Pr = 0.3, M = 0.5, A = 0.2, \beta_1 = \beta_3 = 0.2, \beta_2 = 0.3, t_1 = t_2 = 0.2, N_t = 0.1, N_b = 0.3, E_c = 0.01, S_c = 0.3$ and $N = 2$.

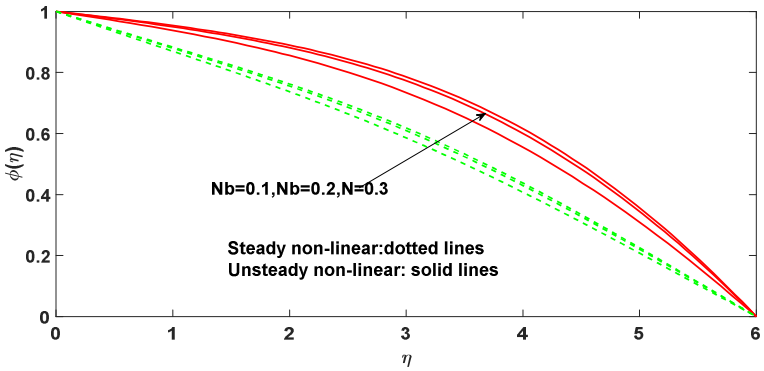

Fig. 8: Effect of the N_b on temperature profile $\phi(\eta)$ with the following fixed values $\Pr = 0.3, M = 0.5, A = 0.2, \beta_1 = \beta_3 = 0.2, \beta_2 = 0.3, t_1 = t_2 = 0.2, N_t = 0.1, N_b = 0.3, E_c = 0.01, S_c = 0.3$ and $N = 2$.

[17] Khan, M., Azeem, W. and Saleh, A. (2016). Non-linear radiative flow of three-dimensional Burgers' nanofluid with new mass flux effect, *International Journal of Heat and Mass Transfer*, 101, 570–576.

[18] Waqas, M., Hayat, T., Farooq, M., Shehzad, S.A. and Alsaedi, A. (2016). Cattaneo-Christov heat flux model for flow of variable thermal conductivity generalized Burgers' fluid, *Journal of Molecular Liquids*, 220, 642–648. doi.org/10.1016/j.molliq.2016.04.086.

[19] Seth, G.S. and Mishra, M.K. (2017). Analysis of transient flow of MHD nanofluid past a non-linear stretching sheet considering Navier's slip boundary condition, *Advanced Powder Technology* 28, 375–384.

[20] Thumma, T., Bég, O.A. and Kadir, A. (2017). Numerical study of heat source/sink effects on dissipative magnetic nanofluid flow from a non-linear inclined stretching/shrinking sheet, *Journal of Molecular Liquids*, 232, 159–173. doi.org/10.1016/j.molliq.2017.02.032.

[21] Nirmala, P.H., Kumari, A.S. and Raju, C.S.K. (2017). Unsteady MHD Couette flow between two parallel plates with uniform suction, *Research J. Science and Tech.*, 9(3), 476–483. doi:10.5958/2349-2988.2017.00083.3.

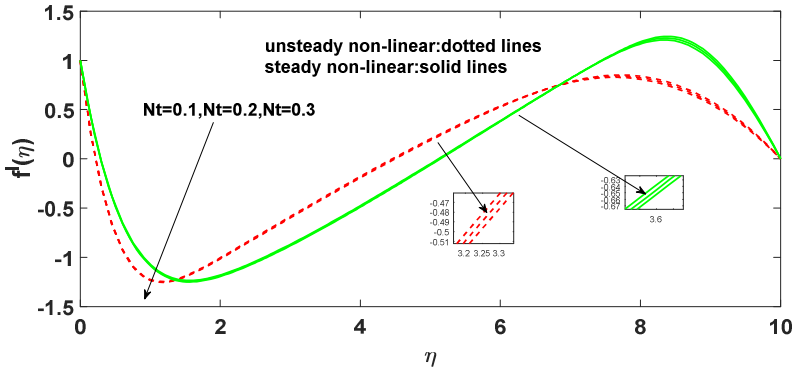

Fig. 9: Effect of the N_t on velocity profile $f'(\eta)$ with the following fixed values $\Pr = 0.2, M = 0.5, A = 0.2, \beta_1 = \beta_3 = 0.2, \beta_2 = 0.3, t_1 = t_2 = 0.2, N_t = 0.1, N_b = 0.3, E_c = 0.01, S_c = 0.3$ and $N = 2$.

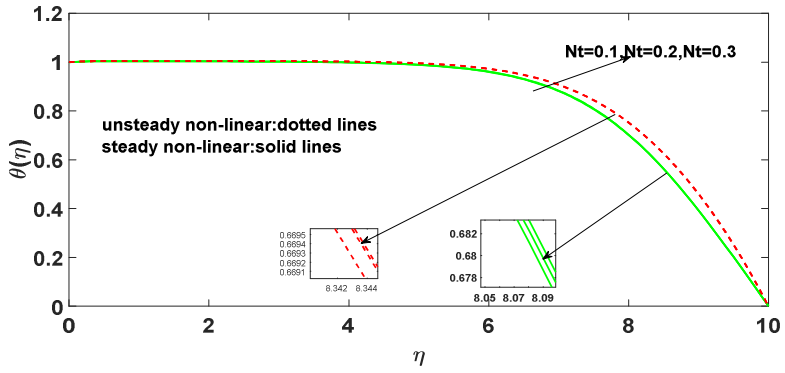

Fig. 10: Effect of the N_t on temperature profile $\theta(\eta)$ with the following fixed values $\Pr = 0.2, M = 0.5, A = 0.2, \beta_1 = \beta_3 = 0.2, \beta_2 = 0.3, t_1 = t_2 = 0.2, N_t = 0.1, N_b = 0.3, E_c = 0.01, S_c = 0.3$ and $N = 2$.

[22] Rashidi, M.M., Yang, Z., Awais, M., Nawaz, M. and Hayat, T. (2017) Generalized Magnetic Field Effects in Burgers' Nanofluid Model, *PLoS ONE*, 12(1): e0168923. doi.org/10.1371/journal.pone.0168923

[23] Nirmala, P.H., Kumari, A.S. and Raju, C.S.K. (2018). An integral Vonkarman treatment of magnetohydrodynamic natural convection on heat and mass transfer along a radiating vertical surface in a saturated porous medium, *Journal of Nanofluids*, 7, 1–9. doi:10.1166/jon.2018.1495.

[24] Adila, N., Azizah, N., Bachok, N., Ishak, A. and Pop, I. (2017). Mixed convection boundary-layer stagnation point flow past a vertical stretching / shrinking surface in a nanofluid, *Applied Thermal Engineering*, 115, 1412–1417. doi.org/10.1016/j.applthermaleng.2016.10.159

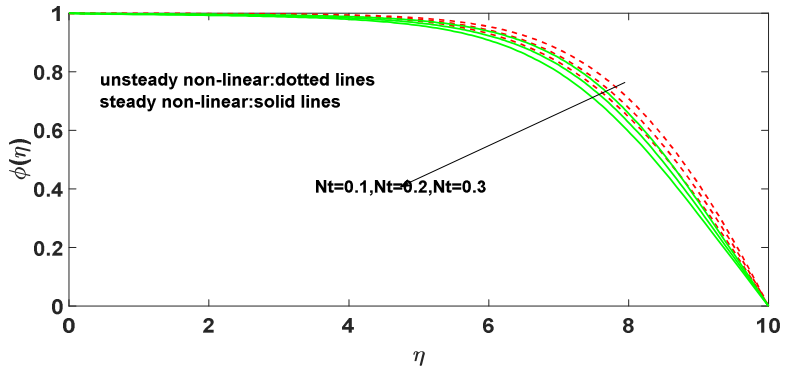

Fig. 11: Effect of the $N_t$on temperature profile $\phi(\eta)$ with the following fixed values $\Pr = 0.2, M = 0.5, A = 0.2, \beta_1 = \beta_3 = 0.2, \beta_2 = 0.3, t_1 = t_2 = 0.2, N_t = 0.1, N_b = 0.3, E_c = 0.01, S_c = 0.3$ and $N = 2$.

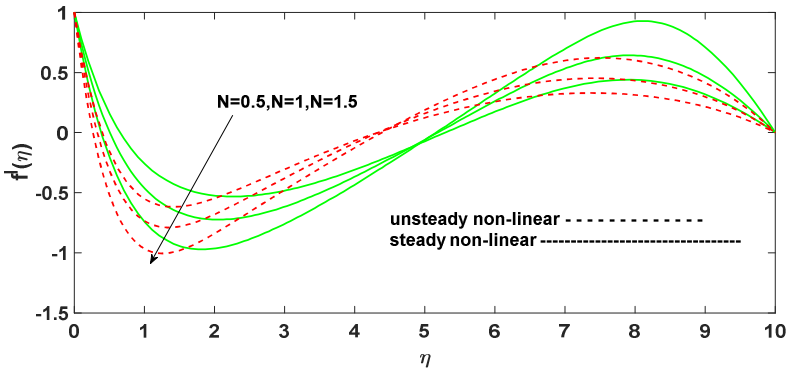

Fig. 12: Effect of the N on velocity profile $f^1(\eta)$ with the following fixed values $\Pr = 0.3, M = 0.5, A = 0.2, \beta_1 = \beta_3 = 0.1, \beta_2 = 0.2, t_1 = t_2 = 0.2, N_t = 0.1, N_b = 0.3, E_c = 0.01, S_c = 0.3$ and $N = 2$.

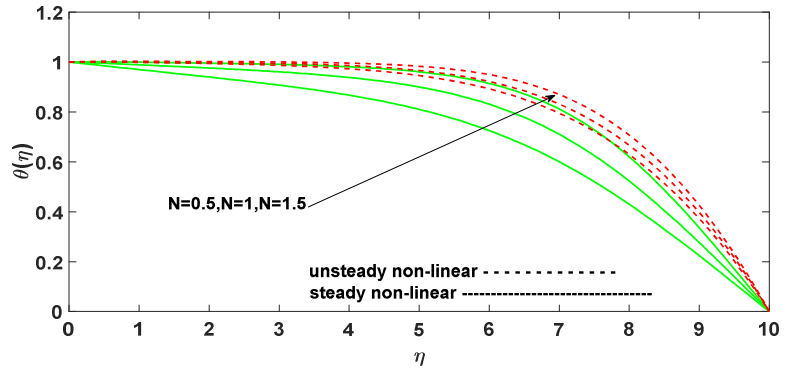

Fig. 13: Effect of the N on temperature profile $\theta(\eta)$ with the following fixed values $\Pr = 0.3, M = 0.5, A = 0.2, \beta_1 = \beta_3 = 0.1, \beta_2 = 0.2, t_1 = t_2 = 0.2, N_t = 0.1, N_b = 0.3, E_c = 0.01, S_c = 0.3$ and $N = 2$.

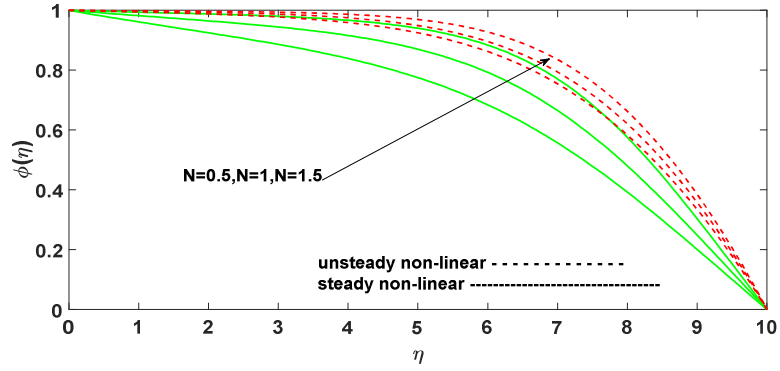

Fig. 14: Effect of the N on temperature profile $\theta(\eta)$ with the following fixed values $\Pr = 0.3, M = 0.5, A = 0.2, \beta_1 = \beta_3 = 0.1, \beta_2 = 0.2, t_1 = t_2 = 0.2, N_t = 0.1, N_b = 0.3, E_c = 0.01, S_c = 0.3$ and $N = 2$.

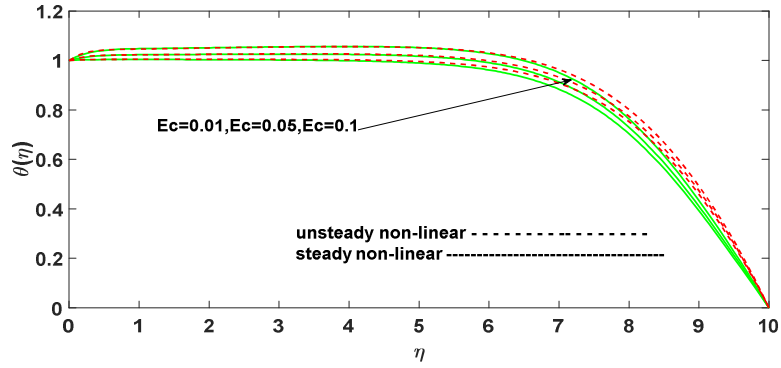

Fig. 15: Effect of the E_C on temperature profile $\theta(\eta)$ with the following fixed values $\Pr = 0.3, M = 0.5, A = 0.2, \beta_1 = \beta_3 = 0.2, \beta_2 = 0.3, t_1 = t_2 = 0.2, N_t = 0.1, N_b = 0.3, E_c = 0.01, S_c = 0.3$ and $N = 2$.

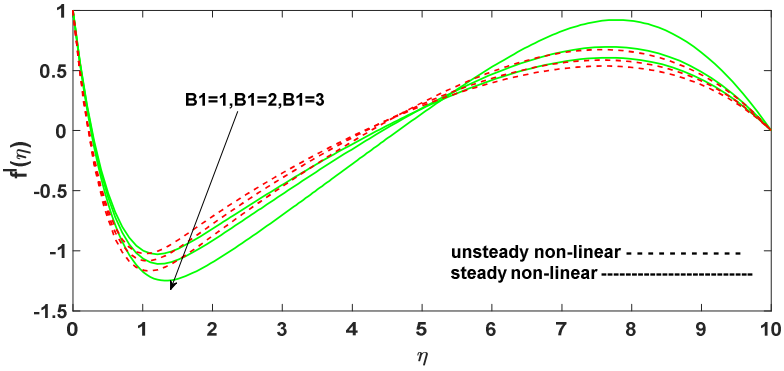

Fig. 16: Effect of the β_1 on velocity profile $f'(\eta)$ with the following fixed values $\Pr = 0.3, M = 0.5, A = 0.2, \beta_1 = \beta_3 = 0.1, \beta_2 = 0.2, t_1 = t_2 = 0.2, N_t = 0.1, N_b = 0.3, E_c = 0.01, S_c = 0.3$ and $N = 2$.

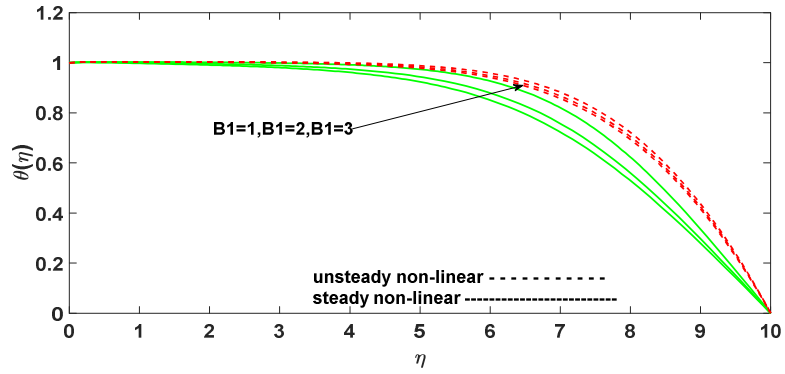

Fig. 17: Effect of the β_1 on temperature profile $\theta(\eta)$ with the following fixed values $\Pr = 0.3, M = 0.5, A = 0.2, \beta_1 = \beta_3 = 0.1, \beta_2 = 0.2, t_1 = t_2 = 0.2, N_t = 0.1, N_b = 0.3, E_c = 0.01, S_c = 0.3$ and $N = 2$.

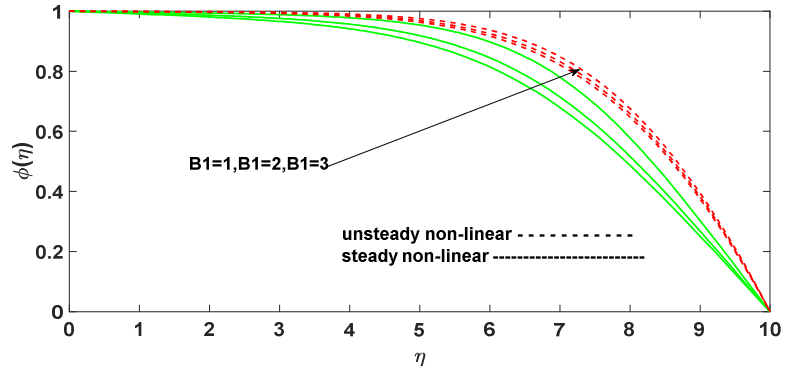

Fig. 18: Effect of the β_1 on concentration profile $\theta(\eta)$ with the following fixed values $\Pr = 0.3, M = 0.5, A = 0.2, \beta_1 = \beta_3 = 0.1, \beta_2 = 0.2, t_1 = t_2 = 0.2, N_t = 0.1, N_b = 0.3, E_c = 0.01, S_c = 0.3$ and $N = 2$.

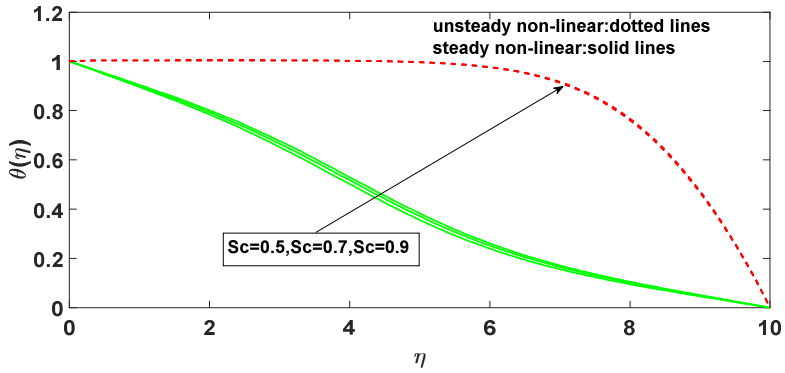

Fig. 19: Effect of the S_C on temperature profile $\theta(\eta)$ with the following fixed values $\Pr = 0.3, M = 0.5, A = 0.2, \beta_1 = \beta_3 = 0.1, \beta_2 = 0.2, t_1 = t_2 = 0.2, N_t = 0.1, N_b = 0.3, E_c = 0.01, S_c = 0.3$ and $N = 2$.

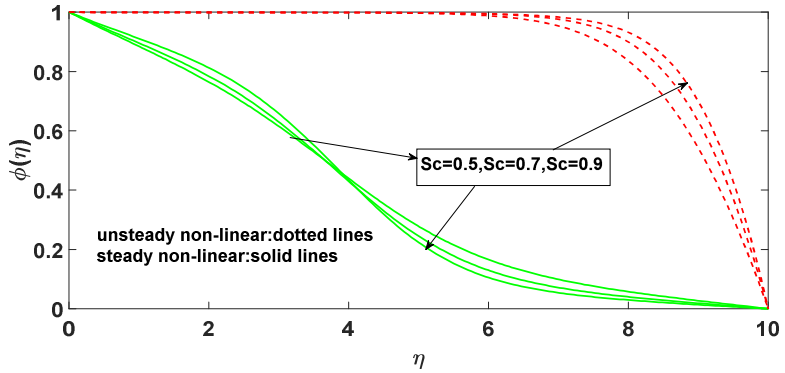

Fig. 20: Effect of the S_C on concentration profile $\theta(\eta)$ with the following fixed values $\Pr = 0.3, M = 0.5, A = 0.2, \beta_1 = \beta_3 = 0.1, \beta_2 = 0.2, t_1 = t_2 = 0.2, N_t = 0.1, N_b = 0.3, E_c = 0.01, S_c = 0.3$ and $N = 2$.